Research Article | Vol. 10, No. 6 | 1 Jun 2019 | BIOMEDICAL OPTICS EXPRESS 3092
Biomedical Optics EXPRESS

Non-invasive depth profiling of the stratum corneum *in vivo* using confocal Raman microscopy considering the non-homogeneous distribution of keratin

MAXIM E. DARVIN,[1,*] CHUN-SIK CHOE,[1,2] JOHANNES SCHLEUSENER,[1] AND JÜRGEN LADEMANN[1]

[1]*Charité-Universitätsmedizin Berlin, Corporate Member of Freie Universität Berlin, Humboldt-Universität zu Berlin, and Berlin Institute of Health, Department of Dermatology, Venerology and Allergology, Center of Experimental and Applied Cutaneous Physiology, Charitéplatz 1, 10117 Berlin, Germany*
[2]*Kim Il Sung University, Ryongnam-Dong, Taesong District, Pyongyang, DPR Korea*
**maxim.darvin@charite.de*

Abstract: Confocal Raman microscopy has a number of advantages in investigating the human stratum corneum (SC) *in vivo* and *ex vivo*. The penetration profiles of xenobiotics in the SC, as well as depth profiles of the physiological parameters of the SC, such as the concentration of water depending on the strength of hydrogen bonds, total water concentration, the hydrogen bonding state of water molecules, concentration of intercellular lipids, the lamellar and lateral packing order of intercellular lipids, the concentration of natural moisturizing factor molecules, carotenoids, and the secondary and tertiary structure properties of keratin are well investigated. To consider the depth-dependent Raman signal attenuation, in most cases a normalization procedure is needed, which uses the main SC's protein keratin-related Raman peaks, based on the assumption that keratin is homogeneously distributed in the SC. We found that this assumption is not accurate for the bottom part of the SC, where the water concentration is considerably increased, thus, reducing the presence of keratin. Our results demonstrate that the bottom part of the SC depth profile should be multiplied by 0.94 in average in order to match this non-homogeneity, which result in a decrease of the uncorrected values in these depths. The correctly normalized depth profiles of the concentration of lipids, water, natural moisturizing factor and carotenoids are presented in this work. The obtained results should be taken into consideration in future skin research using confocal Raman microscopy.

1. Introduction

The stratum corneum (SC), the outermost continuously renewing skin layer, provides the barrier function. It is important for the regulation of water balance and the penetration ability of xenobiotics through the skin. The SC consists of corneocytes (nuclear-free and cytoplasmic organelles-free flattened cells), embedded in the membrane-like ordered intercellular lipid matrix. The corneocytes, which consist of keratin filaments, natural moisturizing factor (NMF) molecules and water, are surrounded by a cornified envelope representing a hard-permeable tough protein/lipid polymer structure [1]. The intercellular lipids (ICL) of the lipid matrix are organized in the form of a classical membrane and their orthorhombic lateral organization represents a highly ordered and very densely packed structure, which is not-permeable for the majority of the non-destructive substances [2–4]. The depth distribution of the lateral organization of ICL is non-homogeneous in the SC, showing a prevalence of orthorhombic over hexagonal ordering in the intermediate SC depths measured *in vitro* [5,6]. The prevalence of the orthorhombic lateral organization in the SC maintains the skin barrier

#363176 https://doi.org/10.1364/BOE.10.003092
Journal © 2019 Received 26 Mar 2019; revised 2 May 2019; accepted 2 May 2019; published 31 May 2019

Biomedical Optics EXPRESS

function [7]. It should be taken into consideration that the structural analysis of ICL using conventional high-resolution methods, such as X-ray diffraction [8], electron diffraction [9], differential scanning calorimetry [10] and electron microscopy [11], are not applicable *in vivo* [12]. For *in vivo* non-invasive analysis of human SC, the application of methods, which are highly sensitive to the chemical composition of substances, such as vibrational spectroscopies (IR and Raman), are irreplaceable. Due to the high absorption by water, IR spectroscopy has a strong depth limitation [13] and therefore, is always used in combination with a tape stripping method [14], which can be considered an invasive procedure. Confocal Raman microscopy (CRM) is applicable for the analysis of approx. 50 µm in depths, at red/infrared excitation, i.e. it is well suited for non-invasive measurements of the entire SC *in vivo* [15]. A recent *in vivo* study using CRM confirmed the non-homogeneous distribution of lateral packing order of ICL, showing the prevalence of the orthorhombic phase in the depth of approx. 30% of the SC depth [16], determining the highest skin barrier function at this depth. These results correlate with further parameters sensitive to the skin barrier function that were determined using *in vivo* CRM, such as the NMF concentration [17], or the hydrogen bonding state of water [18]. One perception from these studies was, that the maximal skin barrier function occurs at the depths 20–40% of the SC thickness. This depth range, should be specially considered for enhancement of the skin barrier function. The analysis of barrier disrupted skin, as e.g. in patients with atopic dermatitis is a further focus using CRM [20].

Penetration profiles of moisturizers [21] and xenobiotics into the SC [22–27] and their influence on skin components [10,28–31] were successfully determined using CRM *in vivo* and *ex vivo*. An increased scientific interest in investigating the SC using CRM has been observed during the last years. One of the main limitations of CRM for the investigation of the SC is the necessity of a normalization procedure in order to compensate for the depth-dependent attenuation of the Raman signal intensity caused by absorption and scattering. In 2001, Caspers and associates [13] proposed a method for the normalization of depth-dependent Raman spectra in the SC on the Raman intensity of keratin, which is the main protein in the SC. The main assumption of this method is the homogeneous distribution of keratin in the entire SC, which has not been proven to the best of our knowledge. This assumption can be true for dry SC biopsies, but changes for *in vivo* skin, whose SC is characterized by a strongly non-homogeneous distribution of water, with the lowest concentration at the superficial layers and highest concentration at the bottom layers of the SC [32]. Water can significantly influence the skin Raman spectra [33,34]. This effect was recently investigated by our group, showing that the concentration of keratin decreased towards the bottom of the SC due to the increase of water, distorting the CRM results in the SC depths exceeding 20% of the SC thickness [35]. This inaccuracy is insignificant in the superficial SC layers (0–20% SC depth), but continuously increases towards the deeper SC layers and is estimated to be on average ≈10% at the bottom of the SC, where the water concentration is maximal.

Thus, in previous CRM studies of the skin *in vivo*, where normalization on keratin was performed, the results obtained for the lower SC depths are slightly overestimated and should be corrected. This is related to the *in vitro* / *ex vivo* / *in vivo* determination of the total water concentration [19,36,37], and the lipid concentration [38]. This applies also to the depth profiles of the NMF concentration in the SC as well as penetration profiles of topically applied substances.

In previous studies, the calculation of physiological parameters of the SC, such as the concentration of water types depending on the hydrogen bond strength (tightly-, strongly-, weakly bound and unbound water types) and the hydrogen bonding state of water molecules [18,37,38], the depth profiles of the lamellar and lateral organization of SC's ICL [16], and the secondary and tertiary keratin folding parameters [19] were determined correctly, as the lipid-, keratin- and water-related Raman peak ratios were always used for calculation, which does not require additional normalization on the keratin concentration.

Biomedical Optics EXPRESS

Here, the SC depth profiles of healthy untreated human skin *in vivo*, which are corrected for the inhomogeneous distribution of keratin in the SC are presented.

2. Materials and methods

2.1. Volunteers

Nine healthy Caucasian volunteers (male and female) aged from 23 to 47 years (mean 34.7 years) were included in the studies. The volunteers were instructed not to use any skin care products on the inner forearms at least 72 h and to exclude contact with water at least 4 h prior to the beginning of the experiments. Before starting the measurements, the volunteers acclimated for 20 minutes in the laboratory at fixed environmental conditions (temperature + 20 °C, relative humidity ≈35%). The measurements were performed on the inner forearm in at least 10 positions.

Before the experiments, the volunteers were informed about the study design and possible risks and had given their written informed consent. Approval for the measurements had been obtained from the Ethics Committee of the Charité–Universitätsmedizin Berlin and all procedures complied with the Code of Ethics of the World Medical Association (Declaration of Helsinki).

2.2. Confocal Raman microscopy (CRM)

The Model 3510 skin composition analyzer dedicated for *in vivo* measurements on the skin (RiverD International B.V., Rotterdam, The Netherlands) has been used in the studies. The excitation wavelength at 785 nm was applied for acquisition in the fingerprint region (FP, 400–2000 cm^{-1}, exposure time 5 s, 20 mW) and at 671 nm for acquisition in the high wavenumber region (HWN, 2000–4000 cm^{-1}, exposure time 1 s, 17 mW). The spatial and spectral resolutions of the CRM were <5 µm and <2 cm^{-1}, respectively. The recorded Raman spectra of the SC were pre-processed by fluorescence background removal and noise filtering using principal component analysis (first four components). The spectra were analyzed based on procedures presented below in sections 2.3–2.6. The utilized CRM was described in detail elsewhere [39]. Characteristic Raman spectra of *in vivo* human SC in the FP and HWN ranges are shown in Fig. 1.

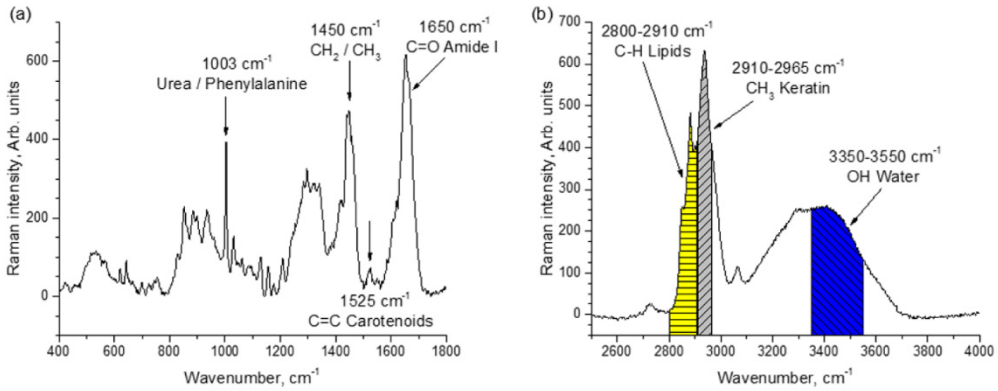

Fig. 1. Characteristic Raman spectra of human SC *in vivo* at 11 µm depth (18 µm SC thickness) in the FP (a) and HWN (b) ranges. The bands at 1003 cm^{-1} (Urea/Phenylalanine), 1450 cm^{-1} (CH_2/CH_3), 1525 cm^{-1} (C = C of carotenoids) and 1650 cm^{-1} (C = C of Amide I), as well as the 2800–2910 cm^{-1} (yellow, C–H of mostly lipids but also keratin), 2910–2965 cm^{-1} (grey, CH_3 of mostly keratin but also lipids) and 3350–3550 cm^{-1} (blue, OH of water) ranges are marked.

Biomedical Optics EXPRESS

2.3. Spectral analysis – determination of the keratin concentration

In the HWN region at 2800–3000 cm^{-1}, lipids and keratin are partly overlaid. In the 2910–2965 cm^{-1} region, keratin has only a minimal contribution of lipids. Therefore, this region is used for the determination of the keratin concentration and further used for the normalization procedure. In order to completely exclude the contribution of lipids to the keratin peak (2910–2965 cm^{-1}), a mathematical algorithm has been developed [16], which takes the contributions of pure substances into account.

Based on the different excitation sources for the FP and HWN regions, it is preferential to use the same region for normalization. Therefore, in some cases, the keratin-related peak at 1450 and 1650 cm^{-1} can potentially be used [35,40].

2.4. Spectral analysis – determination of the lipid concentration

As the Raman HWN range at 2800–3000 cm^{-1} represents the superposition of lipids and keratin, the recently developed algorithm was applied for the determination of the lipid and keratin concentrations [16]. The obtained lipid to keratin ratio represents the normalized concentration of lipids in the SC.

2.5. Spectral analysis – determination of the water (water types) concentration

In the HWN region, the water is presented as a broad Raman peak at ≈2900–3800 cm^{-1}, originating from OH vibrations. In the SC, this peak is overlaid with the Raman peaks of keratin at approx. 3060 and 3300 cm^{-1}. Therefore, the 3350–3550 cm^{-1} region, normalized to keratin (2910–2965 cm^{-1}) is always used for the calculation of the water concentration in the SC [13]. The broad Raman peak of water contains a superposition of OH vibrations characterized by different strengths of hydrogen bonds: “tightly bound” water at ≈3005 cm^{-1}, “strongly bound” water at ≈3280 cm^{-1}, “weakly bound” water at ≈3460 cm^{-1} and “unbound” water at ≈3605 cm^{-1}. The separation of these water types can be achieved by using Gaussian function-based deconvolution in order to exclude an influence of keratin [18,41]. Normally, the concentration of the different water types is presented in % of total water. Therefore, the normalization on keratin is not required.

2.6. Spectral analysis – determination of the skin surface and SC thickness

The skin surface was determined using the “Skin tools 2.0” software (RiverD) [13] at the position of half the maximum keratin intensity. The surface position can be precisely determined using each of the 1003, 1450, 1650 or 2935 cm^{-1} keratin-related Raman peaks [35]. The SC thickness was determined analyzing the water concentration depth profiles (see 2.5). The position where the first derivative reached a value of 0.5, was chosen as the boundary to the stratum granulosum [42]. Hence, the distance between the skin surface and the boundary to the stratum granulosum was defined as the SC thickness. To facilitate the comparison of the results, the individual SC thicknesses were normalized to 100% and interpolated in 10% increments.

2.7. Spectral analysis – determination of the carotenoid and NMF concentration

To calculate the depth profile of the carotenoid concentration in the SC, the non-linear multivariable fitting method available in the “Skin tools 2.0” software was used [22,43,44]. As in the human epidermis, among carotenoids, beta-carotene and lycopene are most abundant [45], a Raman spectrum of beta-carotene in the FP region was used as a representative carotenoid marker to use in the further calculations. Accordingly, depth profiles of the NMF concentration were calculated using “Skin tools 2.0” [13].

Biomedical Optics EXPRESS

2.8. Algorithm for correction of keratin inhomogeneity in the SC

The analysis showed that due to the substantial increase of water concentration in the deeper SC layers, the keratin concentration in the sampling volume of the CRM is decreased. This results in non-homogenous distribution of keratin throughout the SC, which in turn result in an inaccurate normalization procedure. In order to correct this inaccuracy, a mathematical modeling was performed, based on the consideration that the Raman intensity changes depth-dependently due to optical scattering and absorption in the skin [35]. The determined depth-dependent correction factor for keratin-related Raman peaks at 1450, 1650 and 2935 cm^{-1} is 1 (correction is not necessary) at the 0–20% SC depth and starts to decrease non-linearly from 30% SC depth, reaching the lowest value of ≈0.94 (average for 9 volunteers) at the bottom of the SC. In the FP region, the average correction factor between correction factors for 1450 and 1650 cm^{-1} Raman peaks was used.

As, according to Caspers et al. [13], the water concentration is determined in the HWN region as:

$$\frac{W/P}{W/P+R}$$

where W and P are integrated Raman signals of water and protein, and R is a proportionality constant, the water signal is not simply normalized by the keratin signal. Therefore, the correction is non-linear and should be performed according to formula:

$$\frac{(W/P)*corr}{(W/P)*corr+R}$$

where *corr* is a depth-dependent correction factor.

3. Results and discussion

3.1. Lipid concentration

Figure 2 shows the depth profile of the lipid concentration in the SC, determined using the developed correction algorithm, taking the non-homogeneity of the keratin distribution in the SC (solid black line) into consideration and without any corrections under the assumption of homogeneous keratin distribution in the SC (dotted gray line). It is clearly visible that the corrected lipid concentration is slightly, but significantly lower at 40–100% SC depths (p<0.01) than previously reported [37].

Biomedical Optics EXPRESS

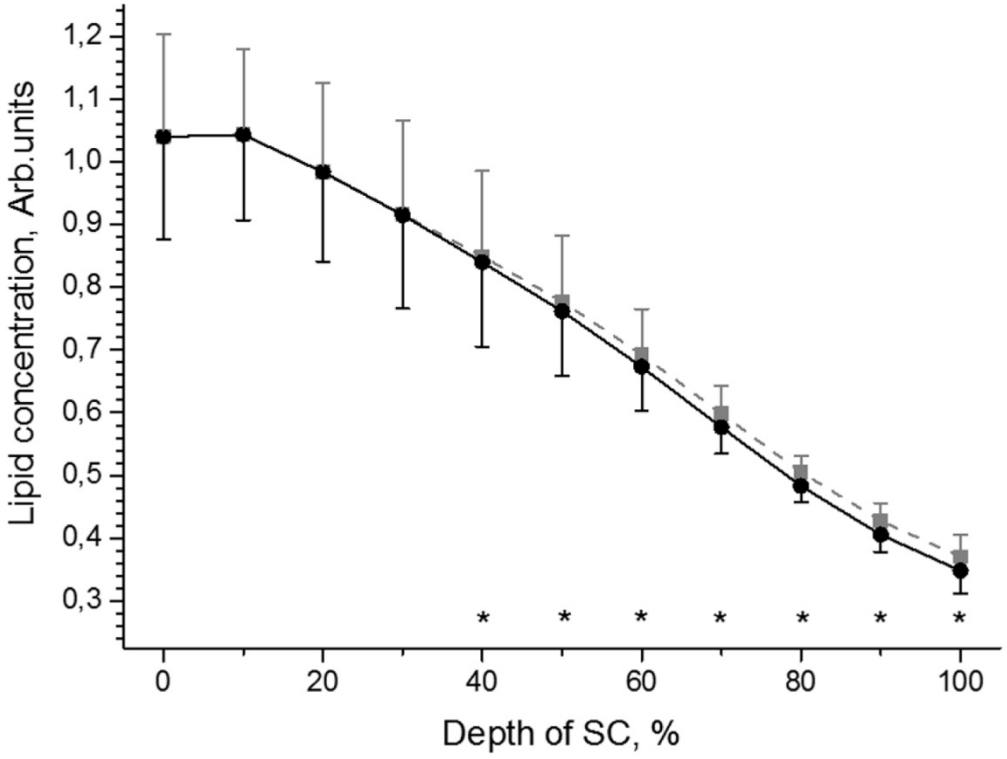

Fig. 2. The *in vivo* SC depth profile of the lipid concentration obtained by taking the non-homogeneity of keratin distribution in the SC into consideration (solid black line) and without any corrections (dotted gray line). For visibility, the error bars, denoting ± 1 standard deviation, are only shown one-sided. "*" represents significant difference (p<0.01) between corrected and uncorrected values.

3.2. Water concentration

Figure 3 shows the depth profile of the total water concentration in the SC, determined using the developed correction algorithm, taking the non-homogenous keratin distribution in the SC into consideration (solid black line) and without any corrections under the assumption of homogeneous keratin distribution in the SC (dotted gray line). It is clearly visible that the corrected concentration of water at the bottom layers of the SC are lower than previously reported [19,37]. The difference is significant for the 50–100% SC depths (p<0.01). As the thickness of the SC is always determined based on the saturation of water concentration at the boundary to the stratum granulosum (see section 2.6), the obtained differences at the bottom SC layers can be attributed to small inaccuracies in determining the SC thickness, which should be further corrected.

Biomedical Optics EXPRESS

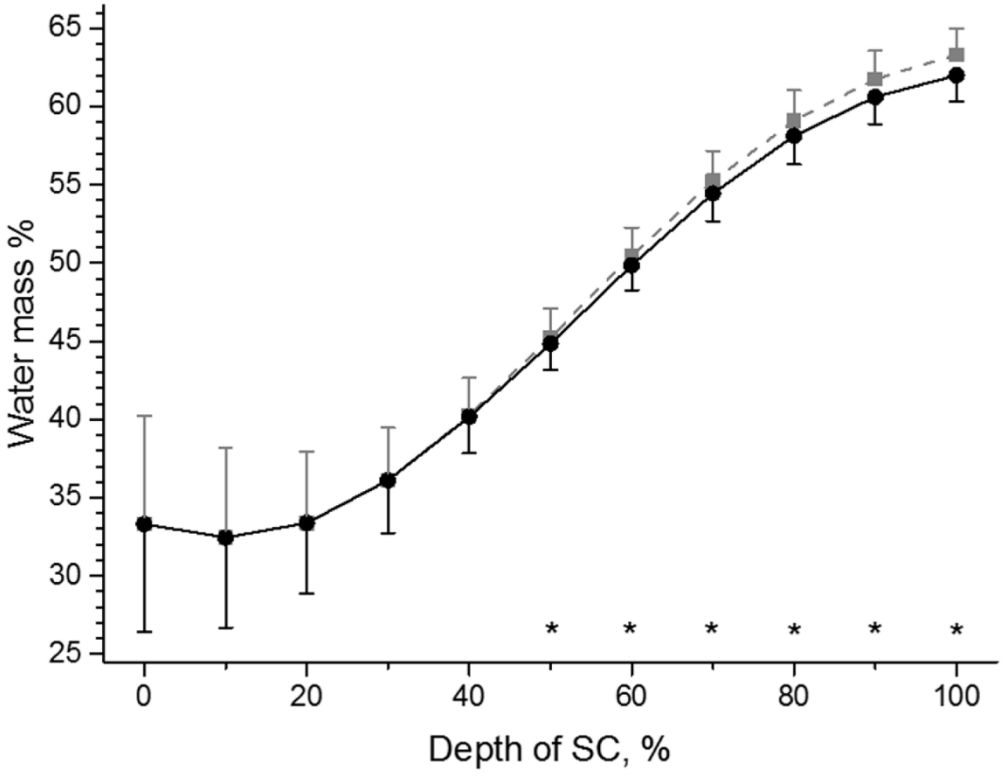

Fig. 3. The *in vivo* SC depth profile of the water concentration in mass % obtained by taking the non-homogeneity of keratin distribution in the SC into consideration (solid black line) and without any corrections (dotted gray line). For visibility, the error bars, denoting ± 1 standard deviation, are only shown one-sided. "*" represents significant difference (p<0.01) between corrected and uncorrected values.

The correction algorithm applies for healthy skin and can be different in case of barrier disrupted skin, for instance, in atopic dermatitis patients, which is characterized by a significantly lower water concentration at the bottom SC layers in comparison to healthy skin [46]. The difference between skin types is mainly manifested by the melanin concentration in the lower epidermis. Therefore, the SC is only expected to vary marginally and hence, an influence of different skin types on the correction factor is not expected to be large. This should be additionally investigated in future studies.

Beneath the SC, in the viable epidermis and in the papillary/reticular dermis, the concentration of total water is comparable to that measured in the bottom layer of the SC [47]. Therefore, the multiplication by the same correction coefficients is also needed for these depths [35] in order to adjust protein inhomogeneity in the sampling volume, used for normalization.

3.3. NMF concentration

Figure 4 shows that the NMF depth profiles in the SC are almost identical and visually independent from the applied correction procedure. The differences are not obvious, because the semi-quantitative concentration of NMF, determined in arb. units, is always below the value 1 in the bottom layers of SC. However, significant differences are obtained for the 40–100% SC depths (p<0.01).

Biomedical Optics EXPRESS

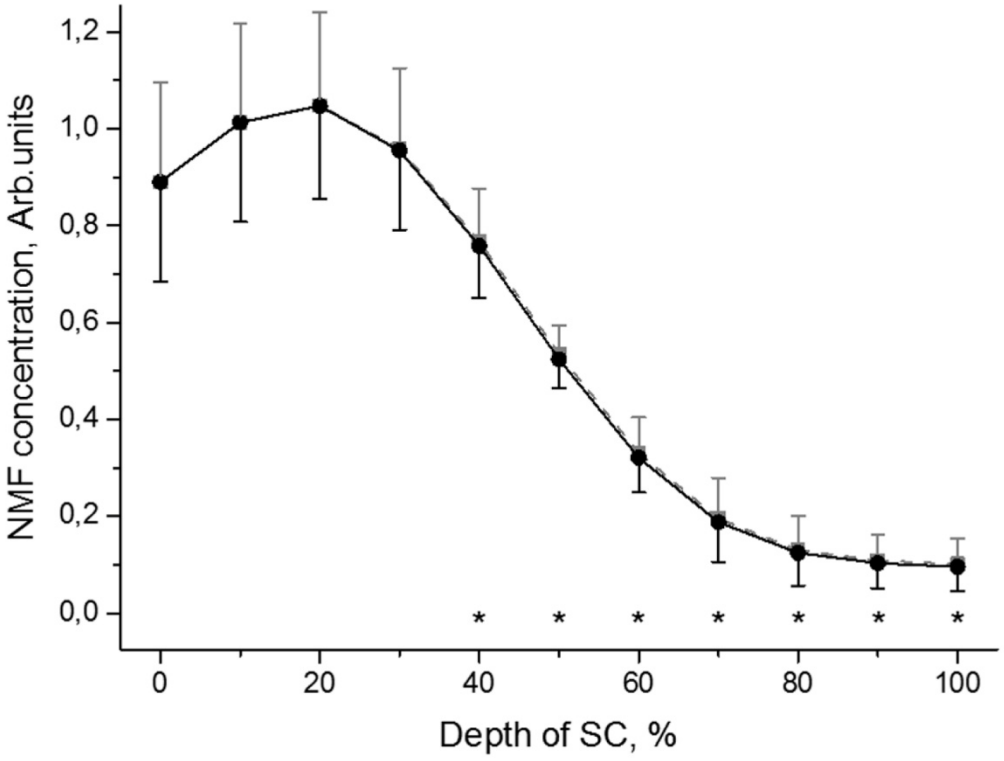

Fig. 4. The *in vivo* SC depth profile of the NMF concentration obtained taking the non-homogenous keratin distribution in the SC into consideration (solid black line) and without any corrections (dotted gray line). For visibility, the error bars, denoting ± 1 standard deviation, are only shown one-sided. "*" represents significant difference (p<0.01) between corrected and uncorrected values.

3.4. Carotenoid concentration

Figure 5 shows the depth profile of the carotenoid concentration in the SC. As can be seen, the carotenoid depth profiles in the SC are almost identical and visually independent from the applied correction procedure, showing highest carotenoid concentration at superficial SC layers and lowest concentration at the bottom SC layers. The profile is similar to previously published results [43,44].

It should be taken into consideration that the non-linear multivariable fitting method, used for the determination of the carotenoid profile, analyzes the entire FP region and is not very precise in analyzing low intensity components. In this respect, the analysis of the 1524 cm^{-1} carotenoid peak AUC can be more precise and serve as a future task.

Biomedical Optics EXPRESS

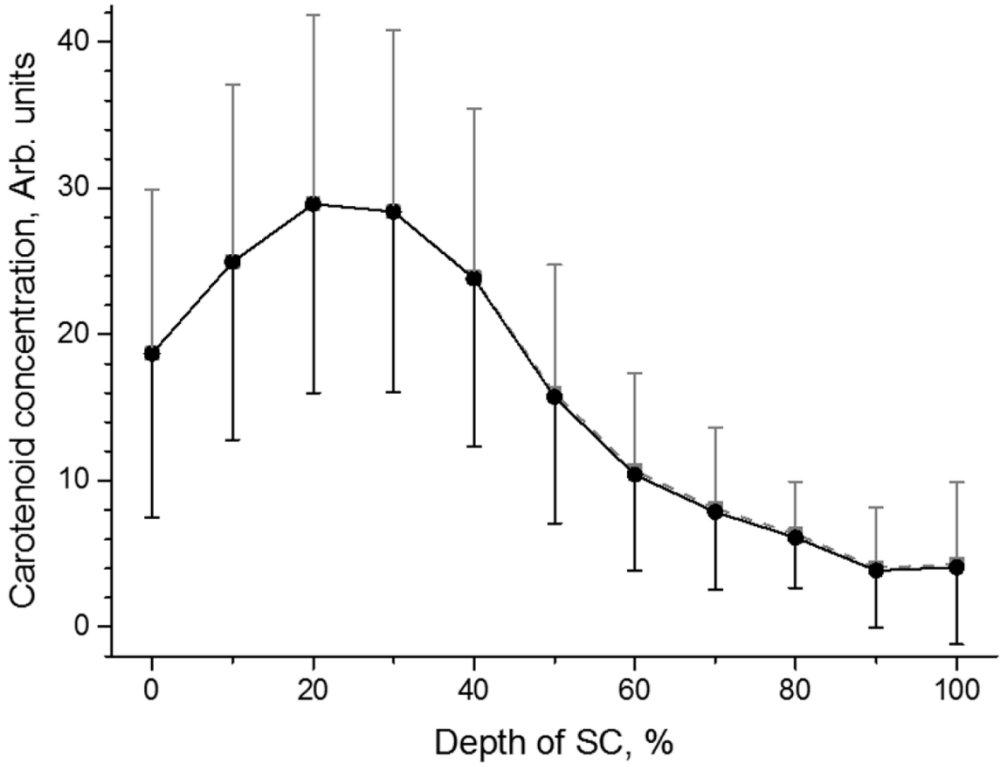

Fig. 5. The *in vivo* SC depth profile of the carotenoid concentration obtained taking the non-homogenous keratin distribution in the SC into consideration (solid black line) and without any corrections (dotted gray line). For visibility, the error bars, denoting ± 1 standard deviation, are only shown one-sided.

4. Conclusion

The non-homogeneous distribution of the water concentration in the SC *in vivo* / *ex vivo* results in a non-homogeneous distribution of the keratin concentration in the sampling volume of the Raman microscope. Until now, the keratin's non-homogeneity was not taken into consideration during normalization procedures. A correction mechanism for the normalization of Raman spectra in the SC, which takes the non-homogeneous distribution of keratin in the SC into consideration, was applied for the first time. The obtained SC depth profiles, where a normalization procedure is required, i.e. the lipid, water, NMF and carotenoid concentrations, are now determined by taking the non-homogenous keratin distribution into account. It is shown that without the application of the correction mechanism, the maximal value of overestimation at the bottom of the SC is approx. 8% by using the keratin peak at 2935 cm^{-1}. The overestimation begins to be visible at the 30% SC depth, which manifests the maximal skin barrier function (20–40%), and reaches statistical significances at 40–100% SC depths. The upper part of the SC depth profile (0–20% SC depth) is similar to the previously presented, uncorrected profile and does not require any correction.

Furthermore, the correction of penetration profiles also results in the decrease of the actual values, i.e. the penetration depth into the SC will be decreased in comparison to uncorrected values.

Biomedical Optics EXPRESS

Funding

German Foundation Centre Essen, Foundation for Skin Physiology (T335), Deutscher Akademischer Austauschdienst.

Acknowledgments

We acknowledge support from the German Research Foundation (DFG) and the Open Access Publication Fund of Charité-Universitätmedizin Berlin.

Disclosures

The authors declare that there are no conflicts of interest related to this article.

References

1. E. Proksch, J. M. Brandner, and J.-M. Jensen, "The skin: an indispensable barrier," Exp. Dermatol. **17**(12), 1063–1072 (2008).
2. J. A. Bouwstra, F. E. Dubbelaar, G. S. Gooris, and M. Ponec, "The lipid organisation in the skin barrier," Acta Derm. Venereol. Suppl. (Stockh.) **208**, 23–30 (2000).
3. F. Damien and M. Boncheva, "The extent of orthorhombic lipid phases in the stratum corneum determines the barrier efficiency of human skin in vivo," J. Invest. Dermatol. **130**(2), 611–614 (2010).
4. K. R. Feingold and P. M. Elias, "Role of lipids in the formation and maintenance of the cutaneous permeability barrier," Biochim. Biophys. Acta **1841**(3), 280–294 (2014).
5. G. S. Pilgram, A. M. Engelsma-van Pelt, J. A. Bouwstra, and H. K. Koerten, "Electron diffraction provides new information on human stratum corneum lipid organization studied in relation to depth and temperature," J. Invest. Dermatol. **113**(3), 403–409 (1999).
6. J. Doucet, A. Potter, C. Baltenneck, and Y. A. Domanov, "Micron-scale assessment of molecular lipid organization in human stratum corneum using microprobe X-ray diffraction," J. Lipid Res. **55**(11), 2380–2388 (2014).
7. J. van Smeden, M. Janssens, G. S. Gooris, and J. A. Bouwstra, "The important role of stratum corneum lipids for the cutaneous barrier function," Biochim. Biophys. Acta **1841**(3), 295–313 (2014).
8. I. Hatta, N. Ohta, S. Ban, H. Tanaka, and S. Nakata, "X-ray diffraction study on ordered, disordered and reconstituted intercellular lipid lamellar structure in stratum corneum," Biophys. Chem. **89**(2-3), 239–242 (2001).
9. H. Nakazawa, T. Imai, I. Hatta, S. Sakai, S. Inoue, and S. Kato, "Low-flux electron diffraction study for the intercellular lipid organization on a human corneocyte," Biochim. Biophys. Acta **1828**(6), 1424–1431 (2013).
10. Z. Zhang and D. J. Lunter, "Confocal Raman microspectroscopy as an alternative to differential scanning calorimetry to detect the impact of emulsifiers and formulations on stratum corneum lipid conformation," Eur. J. Pharm. Sci. **121**, 1–8 (2018).
11. V. Schreiner, G. S. Gooris, S. Pfeiffer, G. Lanzendörfer, H. Wenck, W. Diembeck, E. Proksch, and J. Bouwstra, "Barrier characteristics of different human skin types investigated with X-ray diffraction, lipid analysis, and electron microscopy imaging," J. Invest. Dermatol. **114**(4), 654–660 (2000).
12. S. Kikuchi, T. Aosaki, K. Bito, S. Naito, and Y. Katayama, "In vivo evaluation of lateral lipid chain packing in human stratum corneum," Skin Res. Technol. **21**(1), 76–83 (2015).
13. P. J. Caspers, G. W. Lucassen, E. A. Carter, H. A. Bruining, and G. J. Puppels, "In vivo confocal Raman microspectroscopy of the skin: noninvasive determination of molecular concentration profiles," J. Invest. Dermatol. **116**(3), 434–442 (2001).
14. A. Ezerskaia, N. E. Uzunbajakava, G. J. Puppels, J. de Sterke, P. J. Caspers, H. P. Urbach, and B. Varghese, "Potential of short-wave infrared spectroscopy for quantitative depth profiling of stratum corneum lipids and water in dermatology," Biomed. Opt. Express **9**(5), 2436–2450 (2018).
15. P. E. J. van Erp, M. Peppelman, and D. Falcone, "Noninvasive analysis and minimally invasive in vivo experimental challenges of the skin barrier," Exp. Dermatol. **27**(8), 867–875 (2018).
16. C. Choe, J. Lademann, and M. E. Darvin, "A depth-dependent profile of the lipid conformation and lateral packing order of the stratum corneum in vivo measured using Raman microscopy," Analyst (Lond.) **141**(6), 1981–1987 (2016).
17. S. A. Koppes, P. Kemperman, I. Van Tilburg, F. Calkoen-Kwa, K. A. Engebretsen, G. J. Puppels, P. J. Caspers, and S. Kezic, "Determination of natural moisturizing factors in the skin: Raman microspectroscopy versus HPLC," Biomarkers **22**(6), 502–507 (2017).
18. C. Choe, J. Lademann, and M. E. Darvin, "Depth profiles of hydrogen bound water molecule types and their relation to lipid and protein interaction in the human stratum corneum in vivo," Analyst (Lond.) **141**(22), 6329–6337 (2016).
19. C. Choe, J. Schleusener, J. Lademann, and M. E. Darvin, "Keratin-water-NMF interaction as a three layer model in the human stratum corneum using in vivo confocal Raman microscopy," Sci. Rep. **7**(1), 15900 (2017).

Biomedical Optics EXPRESS

20. L. Verzeaux, R. Vyumvuhore, D. Boudier, M. Le Guillou, S. Bordes, M. Essendoubi, M. Manfait, and B. Closs, "Atopic skin: In vivo Raman identification of global molecular signature, a comparative study with healthy skin," Exp. Dermatol. **27**(4), 403–408 (2018).
21. V. K. Tippavajhala, T. D. Magrini, D. C. Matsuo, M. G. P. Silva, P. P. Favero, L. R. De Paula, and A. A. Martin, "In Vivo Determination of Moisturizers Efficacy on Human Skin Hydration by Confocal Raman Spectroscopy," AAPS PharmSciTech **19**(7), 3177–3186 (2018).
22. P. J. Caspers, A. C. Williams, E. A. Carter, H. G. Edwards, B. W. Barry, H. A. Bruining, and G. J. Puppels, "Monitoring the penetration enhancer dimethyl sulfoxide in human stratum corneum in vivo by confocal Raman spectroscopy," Pharm. Res. **19**(10), 1577–1580 (2002).
23. C. Choe, J. Lademann, and M. E. Darvin, "Analysis of Human and Porcine Skin in vivo/ex vivo for Penetration of Selected Oils by Confocal Raman Microscopy," Skin Pharmacol. Physiol. **28**(6), 318–330 (2015).
24. M. Essendoubi, C. Gobinet, R. Reynaud, J. F. Angiboust, M. Manfait, and O. Piot, "Human skin penetration of hyaluronic acid of different molecular weights as probed by Raman spectroscopy," Skin Res. Technol. **22**(1), 55–62 (2016).
25. C. Alonso, V. Carrer, C. Barba, and L. Coderch, "Caffeine delivery in porcine skin: a confocal Raman study," Arch. Dermatol. Res. **310**(8), 657–664 (2018).
26. L. Miloudi, F. Bonnier, A. Tfayli, F. Yvergnaux, H. J. Byrne, I. Chourpa, and E. Munnier, "Confocal Raman spectroscopic imaging for in vitro monitoring of active ingredient penetration and distribution in reconstructed human epidermis model," J. Biophotonics **11**(4), e201700221 (2018).
27. S. Laing, S. Bielfeldt, K. P. Wilhelm, and J. Obst, "Confocal Raman Spectroscopy as a tool to measure the prevention of skin penetration by a specifically designed topical medical device," Skin research and technology: official journal of International Society for Bioengineering and the Skin (ISBS) [and] International Society for Digital Imaging of Skin (ISDIS) [and] International Society for Skin Imaging (ISSI) (2019).
28. C. Choe, J. Schleusener, J. Lademann, and M. E. Darvin, "In vivo confocal Raman microscopic determination of depth profiles of the stratum corneum lipid organization influenced by application of various oils," J. Dermatol. Sci. **87**(2), 183–191 (2017).
29. A. Y. Sdobnov, V. Tuchin, J. Lademann, and M. E. Darvin, "Confocal Raman microscopy supported by optical clearing treatment of the skin—influence on collagen hydration," J. Phys. D Appl. Phys. **50**(28), 285401 (2017).
30. E. Atef and N. Altuwaijri, "Using Raman Spectroscopy in Studying the Effect of Propylene Glycol, Oleic Acid, and Their Combination on the Rat Skin," AAPS PharmSciTech **19**(1), 114–122 (2018).
31. L. dos Santos, V. K. Tippavajhala, T. O. Mendes, M. G. P. da Silva, P. P. Fávero, C. A. Téllez Soto, and A. A. Martin, "Evaluation of penetration process into young and elderly skin using confocal Raman spectroscopy," Vib. Spectrosc. **100**, 123–130 (2019).
32. P. J. Caspers, G. W. Lucassen, H. A. Bruining, and G. J. Puppels, "Automated depth-scanning confocal Raman microspectrometer for rapid in vivo determination of water concentration profiles in human skin," J. Raman Spectrosc. **31**(8-9), 813–818 (2000).
33. R. Vyumvuhore, A. Tfayli, H. Duplan, A. Delalleau, M. Manfait, and A. Baillet-Guffroy, "Effects of atmospheric relative humidity on Stratum Corneum structure at the molecular level: ex vivo Raman spectroscopy analysis," Analyst (Lond.) **138**(14), 4103–4111 (2013).
34. S. Kim, K. M. Byun, and S. Y. Lee, "Influence of water content on Raman spectroscopy characterization of skin sample," Biomed. Opt. Express **8**(2), 1130–1138 (2017).
35. C. Choe, S. Choe, J. Schleusener, J. Lademann, and M. E. Darvin, "Modified normalization method in in vivo stratum corneum analysis using confocal Raman microscopy to compensate non-homogenous distribution of keratin," J. Raman Spectrosc., (published online ahead of print).
36. J. W. Fluhr, S. Sassning, O. Lademann, M. E. Darvin, S. Schanzer, A. Kramer, H. Richter, W. Sterry, and J. Lademann, "In vivo skin treatment with tissue-tolerable plasma influences skin physiology and antioxidant profile in human stratum corneum," Exp. Dermatol. **21**(2), 130–134 (2012).
37. C. Choe, J. Schleusener, J. Lademann, and M. E. Darvin, "Human skin in vivo has a higher skin barrier function than porcine skin ex vivo-comprehensive Raman microscopic study of the stratum corneum," J. Biophotonics **11**(6), e201700355 (2018).
38. C. Choe, J. Schleusener, J. Lademann, and M. E. Darvin, "Age related depth profiles of human Stratum Corneum barrier-related molecular parameters by confocal Raman microscopy in vivo," Mech. Ageing Dev. **172**, 6–12 (2018).
39. Y. Zhu, C. S. Choe, S. Ahlberg, M. C. Meinke, U. Alexiev, J. Lademann, and M. E. Darvin, "Penetration of silver nanoparticles into porcine skin ex vivo using fluorescence lifetime imaging microscopy, Raman microscopy, and surface-enhanced Raman scattering microscopy," J. Biomed. Opt. **20**(5), 051006 (2015).
40. M. Gniadecka, O. F. Nielsen, S. Wessel, M. Heidenheim, D. H. Christensen, and H. C. Wulf, "Water and protein structure in photoaged and chronically aged skin," J. Invest. Dermatol. **111**(6), 1129–1133 (1998).
41. Q. Sun, "Local statistical interpretation for water structure," Chem. Phys. Lett. **568–569**, 90–94 (2013).
42. J. M. Crowther, A. Sieg, P. Blenkiron, C. Marcott, P. J. Matts, J. R. Kaczvinsky, and A. V. Rawlings, "Measuring the effects of topical moisturizers on changes in stratum corneum thickness, water gradients and hydration in vivo," Br. J. Dermatol. **159**(3), 567–577 (2008).
43. J. Lademann, P. J. Caspers, A. van der Pol, H. Richter, A. Patzelt, L. Zastrow, M. Darvin, W. Sterry, and J. W. Fluhr, "In vivo Raman spectroscopy detects increased epidermal antioxidative potential with topically applied carotenoids," Laser Phys. Lett. **6**(1), 76–79 (2009).

Biomedical Optics EXPRESS

44. M. E. Darvin, J. W. Fluhr, P. Caspers, A. van der Pool, H. Richter, A. Patzelt, W. Sterry, and J. Lademann, "In vivo distribution of carotenoids in different anatomical locations of human skin: comparative assessment with two different Raman spectroscopy methods," Exp. Dermatol. **18**(12), 1060–1063 (2009).
45. T. R. Hata, T. A. Scholz, I. V. Ermakov, R. W. McClane, F. Khachik, W. Gellermann, and L. K. Pershing, "Non-invasive raman spectroscopic detection of carotenoids in human skin," J. Invest. Dermatol. **115**(3), 441–448 (2000).
46. L. Zhang, T. Cambron, Y. Niu, Z. Xu, N. Su, H. Zheng, K. Wei, and P. Ray, "MCR Approach Revealing Protein, Water, and Lipid Depth Profile in Atopic Dermatitis Patients' Stratum Corneum via in Vivo Confocal Raman Spectroscopy," Anal. Chem. **91**(4), 2784–2790 (2019).
47. A. Y. Sdobnov, M. E. Darvin, J. Schleusener, J. Lademann, and V. V. Tuchin, "Hydrogen bound water profiles in the skin influenced by optical clearing molecular agents-Quantitative analysis using confocal Raman microscopy," J. Biophotonics **12**(5), e201800283 (2019).